Characteristics of Underwater Ambient Noise at a Proposed Tidal Energy Site in Puget Sound

Christopher Bassett
Jim Thomson
Brian Polagye
Northwest National Marine Renewable Energy Center
University of Washington
Seattle, WA 98115
email: cbassett@u.washington.edu

***Abstract*—Ambient underwater acoustics data are presented for one year at a potential tidal energy site in Admiralty Inlet, WA (USA) with maximum currents exceeding 3 m/s. The site, at a depth of approximately 60 meters, is located near shipping lanes, a local ferry route, and a transit area for many cetacean species. A key finding is that the statistical distribution of total sound pressure levels are dependent on tidal currents at the site. Pseudosound, cobbles shifting on the sea bed, and vibrations induced by forces on the equipment are possible explanations. Non-propagating turbulent pressure fluctuations, termed pseudosound, can mask ambient noise, especially in highly energetic environments suitable for tidal energy development. A statistical method identifies periods during which changes in the mean and standard deviation of the one-third octave band sound pressure levels are statistically significant and thus suggestive of pseudosound contamination. For each deployment, recordings with depth averaged tidal currents greater than 1 m/s are found to be contaminated, and only recordings with currents below this threshold are used in the subsequent ambient noise analysis.**

Mean total sound pressure levels (0.156 - 30 kHz) over all recordings are 117 dB re 1μPa. Total sound pressure levels exceed 100 dB re 1μPa 99% of the time and exceed 135 dB re 1μPa 4% of the time. Commercial shipping and ferry traffic are found to be the most significant contributors to ambient noise levels at the site, with secondary contributions from rain, wind, and marine mammal vocalizations. Post-processed data from an AIS (Automatic Identification System) receiver is used to determine the location of ships during each recording. Referencing 368 individual recordings with the distance between the ferry and the site obtained from AIS data, the source level of the ferry is estimated to be 179 $\pm$ 4 dB re 1μPa at 1m with a logarithmic spreading loss coefficient of 18.

***Index Terms*—Underwater acoustics, ambient noise, pseudosound, tidal energy**

I. Introduction

The location of the proposed tidal energy pilot project is Eastern Admiralty Inlet, Washington State. The majority of tidal exchange between the Strait of Juan de Fuca and Puget Sound occurs in Admiralty Inlet. As a result, strong tidally driven currents make the site attractive for tidal hydrokinetic energy development. The survey area is a 1.5 km x 1.0 km rectangle that is roughly aligned with the principal axis of the flow in and out of Puget Sound. Figure 1 identifies the Puget Sound, Admiralty Inlet, and the location of the survey area.

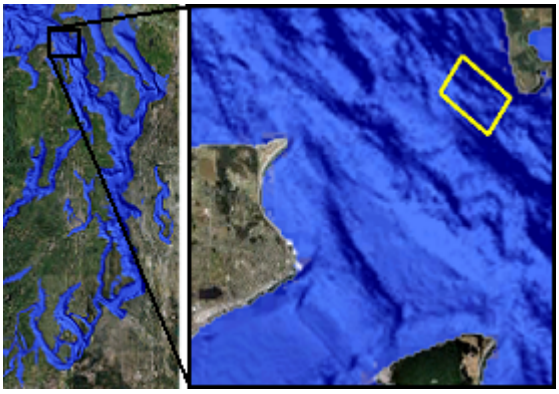

Fig. 1: Puget Sound (left inset), Admiralty Inlet (right inset), and survey area (yellow rectangle in the right inset).

Passive acoustics data are obtained by deploying an instrumentation tripod on the sea floor at the site for four consecutive three-month periods. After three months, the tripod is recovered, the data are downloaded, and the tripod is redeployed. The tripod contains a hydrophone for passive acoustic monitoring, an Acoustic Doppler Current Profiler for measuring currents throughout the water column, PODs for recording cetacean echolocations, and a Conductivity, Temperature, Depth, and Dissolved Oxygen sensor (CTDO). The dates, coordinates, and depths of the four deployments reported in this document are included in Table I.

TABLE I: Deployment coordinates and depth

Deployment	Lat. (°N)	Long. (°W)	Depth (m)
1: 5/20/09 - 8/3/09	48.1509	122.688	54
2: 8/5/09 - 11/11/09	48.1489	122.691	61
3: 11/12/09 - 1/29/10	18.1477	122.690	62
4: 2/12/10 - 5/4/10	48.1501	122.686	51

II. Literature Review

Underwater noise can be attributed to different categories of sources: Natural physical processes, biological sources, and anthropogenic sources. A summary of source levels and

Fig. 2: Deployment Tripod.

frequencies at which common sources affect ambient noise are included in Wenz (1962) . Common contributors to the ambient noise budget at frequencies included in this study include wind, precipitation, ship traffic, and biological sources.

Wind over the surface of the ocean creates shear stresses that can result in breaking waves. Breaking waves at the air-sea interface entrain acoustically active bubbles which produce sound at frequencies dependent on the bubble diameter [2]. The underwater noise spectrum produced by wind has a constant negative slope of approximately 16 dB/decade from 1 to 50 kHz [2]. Although sea state is commonly used to describe surface conditions, wind speed is better correlated with underwater noise levels than sea state [3]. Surf noise may also impact the ambient noise spectrum due to the proximity of the site to the shore. Surf generates noise between 100 Hz and 20 kHz at the interval of waves breaking on the shore (Deane, 2000).

Light rainfall ($<$ 2.5 mm/hr) produces underwater noise through two unique mechanisms - impact noise related to the kinetic energy of the droplet and a louder noise associated with damped oscillations of an entrained microbubble. The resulting acoustic signature is of light rainfall is a broad spectral peak between 12 - 25 kHz, with an average of 15 kHz, due to the resonant frequency of the entrained microbubbles [4]. Increased wind speeds during periods of light precipitation decrease the peak spectral levels and increase the frequency of the peak spectral level [5].

The most common source of anthropogenic noise in Admiralty Inlet is ship traffic. Ship noise is attributed to mechanical noise, flow over the hull, cavitation due to the propeller, and through the use of active acoustic technologies (e.g. depthsounders). Military and commercial sonars have a wide range of peak frequencies from low ($<$ 1 kHz) to very high ($>$ 200 kHz). Source levels across the peak frequency range for different sonars reach 235 dB [6]. Cavitation due to a pressure drop across the propeller creates broadband noise [6]. Low frequency tonal contributions to the ambient noise spectra are related by multiples of the number propeller blades multiplied by the revolutions per second [7]. Mechanical noise is a result of the firing rate of the onboard diesel engines, gearing, pumps, and other mechanical equipment. Hydrodynamic noise from the flow over the hull of the ship contributes to broadband radiated noise, particularly at high velocities [6].

Every vessel has a unique acoustic signature and source level related to ship speed, the condition of the vessel, vessel load, and on-board activities [8]. Source levels for ship traffic range from 150 dB for small fishing vessels to 195 dB for super tankers [6], [9]. Peak spectral levels for shipping traffic occur at less than 500 Hz with substantial tonal contributions as low as 10 Hz [10].

Oceanic turbulence and turbulent pressure fluctuations in the hydrophone boundary layer can be recorded by hydrophones. If sufficiently large, turbulent pressure fluctuations can mask propagating ambient noise signals. In coastal environments, pressure fluctuations due to turbulence advected over a hydrophone have been measured. Hydrophone data obtained in Narragansett Bay, Rhode Island in the one-third octave band centered at 25 Hz show increased sound pressure levels attributed to turbulence during periods of strong tidal currents [11]. Turbulent pressure fluctuations are measured by hydrophones but are not propagating sound and are therefore referred to as *pseudosound*. A small radiated noise component is produced by turbulence but the contributions to the noise budget are minimal because they radiate at a low efficiencies and decay rapidly with distance [12].

Interactions between the turbulent pressure field and the hydrophone also create pseudosound. It has been shown that pressure fluctuations in the hydrophone boundary layer are greater in magnitude than pressure fluctuations of the turbulent field alone and that the impacts of boundary layer fluctuations are greatest at low frequencies and dependent on hydrophone geometry [13]. Attempts to describe wind screen noise on microphones using non-dimensional parameters have been successful but similar non-dimensionalization of hydrophone flow-noise were less successful. Possible explanations for the disparities include differences in the construction of hydrophones as well as susceptibility of hydrophones to vibrations caused by swift underwater currents [14]. One method employed to identify pseudosound is calculating signal coherence, a frequency space measure of the correlation of two independent signals. For propagating sound the coherence between two hydrophones separated by a short distance will be high but the coherence of pseudosound measurements will be low due to the chaotic nature of turbulence. The method requires two hydrophones and has been employed in studies

of ambient noise to identify periods of pseudosound [15].

III. Methodology

Passive acoustic recordings are obtained using a Loggerhead DSG data acquisition system and logger. The data logger is contained in a pressure case to provide a platform for remote sensing. The data logger is connected to a Hi-Tech Instruments custom hydrophone with a sensitivity of -185.5 dB-V/μPa. A preamplifier applies a 10x voltage to the data before recording the 16-bit digital signal for effective sensitivity of -165.5 dB-V/μPa. The frequency response is approximately flat ($\pm$ 3 dB) from 10 Hz to 30 kHz. The data are logged on a 16 GB SD card which is recovered upon retrieval of the tripod.

Acoustics data are recorded every ten minutes throughout each of the four deployments. The sampling frequency during the deployments is 80 kHz. During the first two deployments recordings are 60 seconds long. A subset of each recording, 410 of every 4096 data points, are retained as a form of data compression. During the third and fourth deployments the recordings sampling continuously for 8 seconds. Table II is a summary of the deployment configurations and the bandwidth of the acoustic spectra obtained from the analysis.

TABLE II: Sampling configuration and resulting bandwidth by deployment

Deployment	1	2	3	4
Data Points	410*	410*	4096	4096
Overlap (%)	-	-	50	50
Length (sec.)	60	60	8	8
Bandwidth (Hz)	156.25	156.25	19.53	19.53

*The 410 data points are a subset of a signal sampled at 80 kHz. The 410 point recording is zero-padded to 512 data points before processing the signal.

In underwater sound the standard reference pressure is 1 μPa in contrast with the 20 μPa reference pressure that is used in air. As a result, all decibel levels throughout this document will refer to decibels with respect to 1 μPa. The total sound pressure level is defined as root mean square (rms) pressure squared divided by the reference pressure squared (Equation 1). The total SPL is an important measure of underwater sound across all frequencies but does not provide any information about the frequency content of the signal.

$$SPL\ (dB\ re\ 1\mu Pa)\ =\ 20\ log_{10}\left(\frac{p_{rms}}{p_{ref}}\right) \qquad (1)$$

The pressure time series is converted to acoustic spectra and sound pressure levels over the frequencies bands of interest using standard signal processing methods covered in texts such as Priestley (1981) and Bracewell (2000). The signals are broken into windows that are subsets of the full signal. A Hann function and correction factor are applied to the window in order to satisfy Parseval's Theorem. A Fast Fourier Transform (FFT) algorithm converts the signal from time to frequency space. Pressure spectral densities (PSD) are calculated by calculating the magnitude squared of the FFT and normalizing it by the sampling frequency (f_s) and number of samples in the signal (N). The spectra are then converted to decibels. The resulting units for pressure spectral density are dB re 1 μPa^2/Hz. Sound pressure levels (dB re 1 μPa) are calculated by integrating the pressure spectral density curve over the frequency bands of interest.

$$PSD\ (dB\ re\ 1\mu Pa^2/Hz)\ =\ \frac{2\ |FFT|^2}{f_s N} \qquad (2)$$

$$SPL\ (dB\ re\ 1\mu Pa)\ =\ \int_{f_1}^{f_2} PSD\ df \qquad (3)$$

Three ancillary data sets are used in conjunction with acoustics data to aid in the interpretation of the results. Daily and hourly precipitation data are obtained from the Washington State University Agricultural Weather Network station on Whidbey Island approximately 3.5 miles NNE of the site. Ship traffic information is obtained using an Automatic Identification System (AIS) receiver installed at Fort Casey State Park. Data are post-processed using a Python script and are used to analyze the location of ships and corresponding increases in sound pressure levels at the site. Information on marine mammals, in particular Souther Resident killer whales, (SRKW) in the vicinity of the site are obtained from the Orca Network website and private correspondence with Dr. Scott Veirs of Beam Reach Marine Science and Sustainability School.

IV. Results

A. Velocity Dependence and Pseudosound

Increases in sound levels measured during periods of high current as a result of oceanic turbulence, turbulence in the hydrophone boundary layer, wakes induced by the tripod and other equipment, and vibrations or self-noise induced by forces on the equipment can contaminate true ambient noise statistics measured at the site. A scatter plot of the total SPL versus the depth averaged velocity for the May, 2009 to August, 2009 deployment (Figure 3) demonstrates a clear dependence of recorded SPLs on velocity. One method of identifying pseudosound is to calculate signal coherence, a measure of the correlation of two signals in frequency space. If the distance between two hydrophones is small coherence will be high for a propagating sound. If pseudosound is contaminating the signal coherence will be low due to the chaotic nature of turbulence.

With only one hydrophone, calculating signal coherence is not possible so a method for identifying recordings potentially contaminated by pseudosound is implemented. The data are analyzed and statistics compared in one-third octave band frequency bins and 0.25 m/s velocity bins. Figure 4 includes the probability density functions (PDF) for the data as well as plots of normal distributions with the measured means and standard deviations obtained from the data set for two different velocities. The distribution around slack tide (0 - 0.25 m/s) has a mean of 95 dB and a standard deviation of 8 dB. The

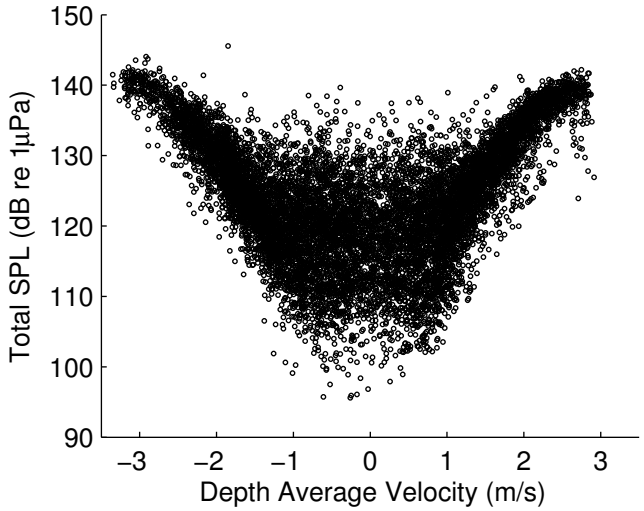

Fig. 3: Total sound pressure level (0.156 - 30 kHz) versus depth averaged velocity for the May, 2009 - August, 2009 deployment.

distribution during moderately strong flood tides (2.0 - 2.25 m/s) has a mean of 104 dB and a standard deviation of 4 dB.

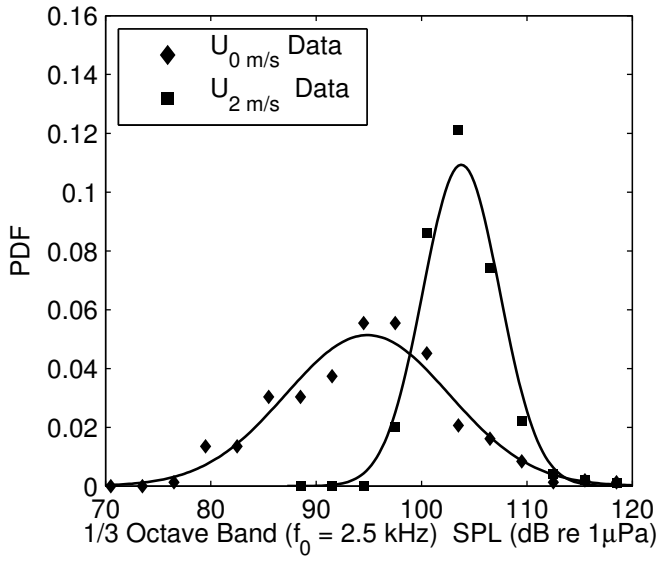

Fig. 4: Probability density functions for two velocity bins in the 1/3 octave band centered at 2.5 kHz from the November, 2009 to February, 2010 deployment show that SPLs in each frequency and velocity bin follow a normal distribution. The solid lines plot a normal distribution for data with the means and standard deviations calculated from the data set.

Gaussian distributions of 1/3 octave band SPLs in each 0.25 m/s velocity bin suggest moment analysis as a method for identifying statistical shifts with increased currents. The means for the slack tide bins (-0.25 m/s to 0.25 m/s) are subtracted from all other velocity bins to show the mode shifting with velocity as represented by Equation 4. For periods uncontaminated by pseudosound Equation 4 is approximately one. A measure of the second moment, a normalized standard deviation is calculated by Equation 5. The standard deviation is normalized at each bin by the standard deviation of the slack tide bins at the same frequency. For samples uncontaminated by pseudosound Equation 5 is approximately equal to one. As depth averaged velocity increases, the normalized standard deviation decreases so the results from Equation 5 decrease. Only velocity bins in which there is no significant shift in mean or normalized standard deviation at any frequency are used for ambient noise analysis. Proper one-third octave bands cannot be resolved under 1.25 kHz for the first two deployments so the closest approximations are used.

TABLE III: Total number of acoustic samples and the number uncontaminated by pseudosound

Deployment	Total Recordings	Uncontaminated Recordings	Percent Uncontaminated
1	10847	4567	42.1
2	13951	5495	39.4
3	12272	5989	48.8
4	10886	4215	38.7
All	47957	20266	42.3

$$\Delta\overline{SPL}_{f,v} = \overline{SPL}_{f,v} - \overline{SPL}_{f,0} \tag{4}$$

$$\sigma_{normalized} = \frac{\sigma_{f,v}}{\sigma_{f,0}} \tag{5}$$

A graphical representation of the statistics used to select uncontaminated data for the four deployments is included in Figure 5. The top windows show the shifting means and the bottom windows show the shifting normalized standard deviation for each frequency and velocity bin . The threshold chosen for uncontaminated data was depth-averaged currents under 1 m/s. The total number of recordings during each deployment, the number of surveys uncontaminated by pseudosound, and the percentage uncontaminated by pseudosound is included in Table III. Overall, 20266 of the 47957 recordings are used in ambient noise analysis.

B. Ambient Noise Spectra, Statistics, and Permanent Noise

After removing all contaminated data, ambient noise statistics are calculated and the impact of noise sources on underwater noise levels are analyzed using the ancillary data sets. Figure 6 includes four different spectra that reflect the different conditions at the site. The spectrum of ship traffic recorded with a ship approximately 2 km from the site in the Northbound shipping lane shows the broadband increases in spectral levels. The rain recording is quiet relative to the recording of ship traffic but has the wide spectral peak centered at 15 kHz that is consistent with light rainfall. The quiet recording is representative of periods with no identifiable sources in the area. The biological noise recording is spectrum of a killer whale (*Orcinus Orca*) vocalization near the site.

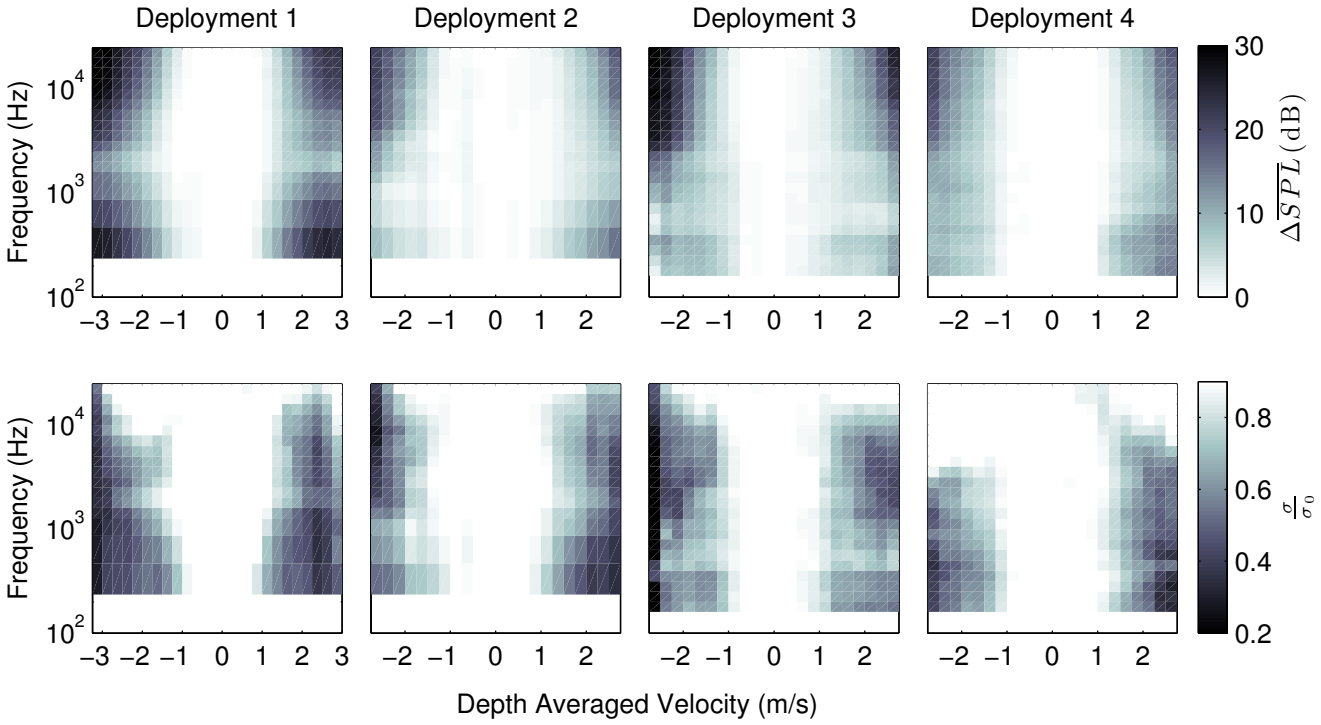

Fig. 5: Frequency versus depth averaged velocity where the gray scale represents mean one-third octave band sound pressure level shifts in the top panel and normalized standard deviation shifts in the bottom panel.

Total sound pressure levels (0.02 - 30 kHz) are 138 dB for the ship recording, 112 dB for the rain recording, and 105 dB for the quiet recording. Before and during the orca vocalization the total SPLs are 109 and 116 dB respectively.

A spectrogram is a time series representation of acoustic spectra where the x-axis is the time, the y-axis is the frequency, and the color is pressure spectral density. Figure 7 includes spectrograms for November 5, 2009 and November 6, 2009. Both spectrograms show broadband increases in pressure spectral density associated with pseudosound between 02:00 and 04:00 and again from 20:00 to 22:00. While not used in the ambient noise analysis these periods are included in the spectrograms to have a complete time series for the days and to demonstrate that pseudosound is sufficiently loud to mask other ambient noises. Periodic increases lasting up to 30 minutes are seen on both days and are a result of shipping traffic in Admiralty Inlet. On November 5, local ferry traffic was cancelled for maintenance of the ferry. The normal ferry schedule resumed on November 6. The additional broadband increases seen throughout the day on November 6 that are not present on November 5 are a result of ferry traffic.

Cumulative probability distribution functions of the total sound pressure level (0.156 - 30 kHz) are constructed for each deployment and the entire data set (Figure 8). The mean total sound pressure levels for the four deployments in chronological order are 118, 118, 116, 117 dB respectively. The mean total SPL for all deployments is 117 dB. The

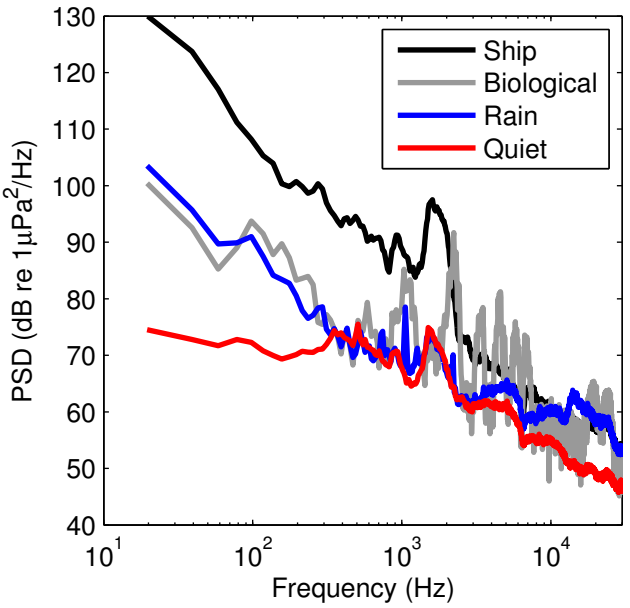

Fig. 6: Acoustic spectra demonstrating the variability of ambient noise conditions and sources at the site.

distributions are Gaussian with standard deviations of 7, 8, 8, and 7 dB respectively. The minimum and maximum recorded

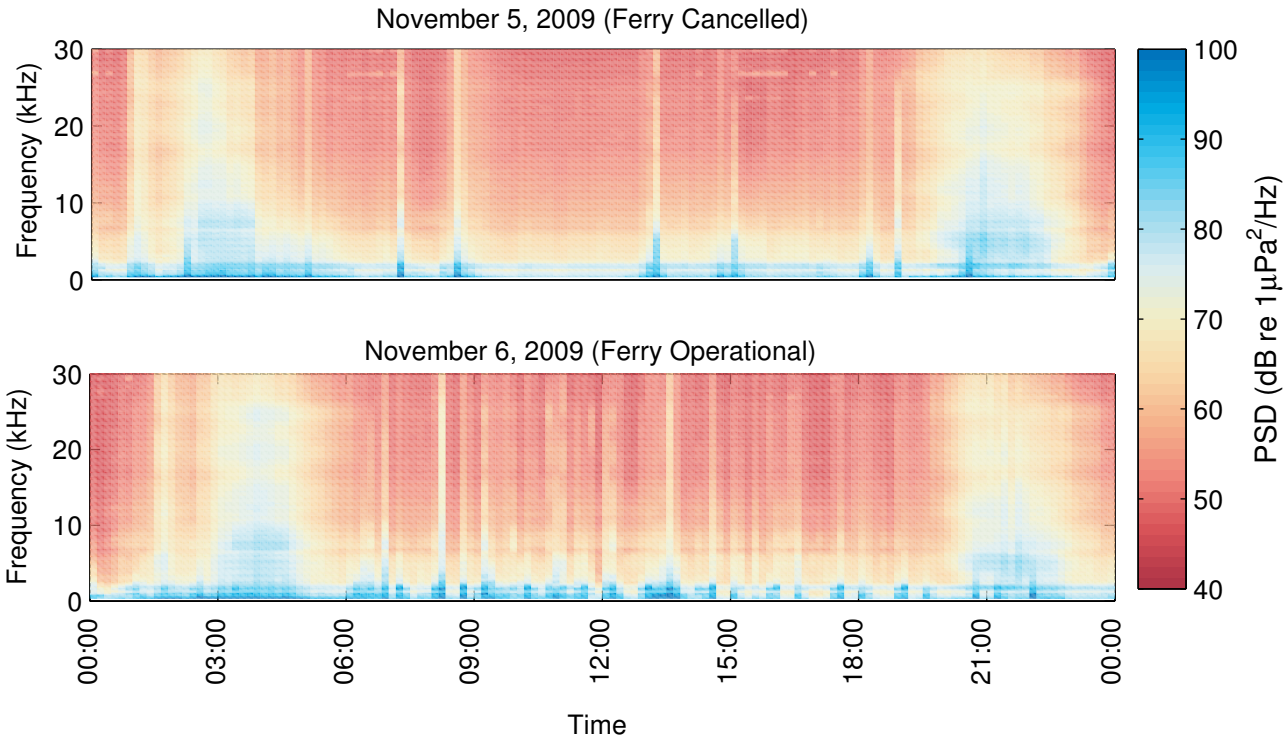

Fig. 7: Spectrograms for November 5 and 6, 2009 show variability caused by pseudosound, shipping traffic, and ferry traffic.

total SPLs are 94 dB during the third deployment and 144 dB during the second deployment.

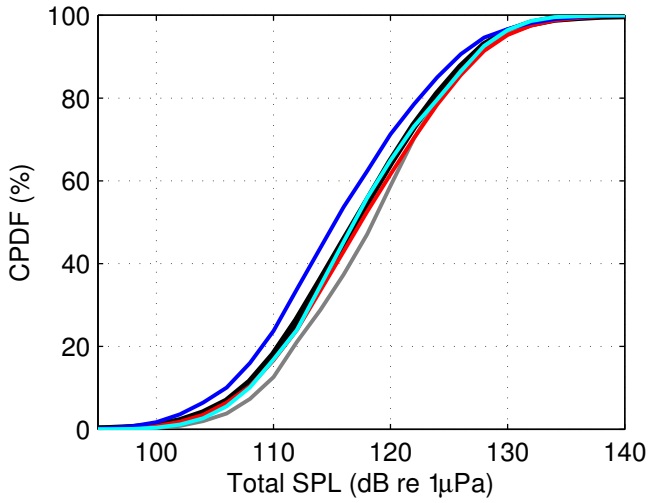

Fig. 8: Cumulative probability density function of total sound pressure level (0.156 - 30 kHz) for the four deployments. Plot lines colors correspond to the following deployments: All data-black, 1-gray, 2-red, 3-blue, 4-light blue

The lowest level of background noise encountered at a site can be defined as the permanent noise [18]. Due to the low duty-cycle, long time series, and sparse data set identifying noise sources near the site, the permanent noise at the site has been defined as the mean of the lowest 1% of total SPLs recorded at the site. The permanent noise level are 98, 99, 98, and 99 dB for the deployments in chronological order. Permanent noise levels calculated in one-third octave bands for each deployment are plotted in Figure 9. Permanent noise in one-third octave band sound pressure levels range from 80 dB in the frequency band centered at 1.25 kHz during the May, 2009 to August, 2009 deployment to 91 dB in the frequency band centered at 160 Hz during the the February, 2010 to May, 2010 deployment.

C. Ferry Noise

The Keystone/Port Townsend ferry is used as a source of opportunity to estimate spreading losses from an acoustic source at the site. The ferry source level at one meter and spreading losses are calculated by plotting the total SPL versus the log of the distance between the ferry and the hydrophone. The y-intercept of the best line of fit is the estimated source level at one meter and the slope of the line is the empirically derived geometric spreading. A least squares linear regression is used to calculate the 95% confidence intervals.

Six weeks of AIS data obtained between December 13, 2009 and January 15, 2010 and January 24, 2010 to January 31, 2010 are combined with acoustic recordings for the estimates. Recordings when currents exceed 1 m/s are removed to avoid contamination by pseudosound. All recordings in which another vessel is known to be within 9 km (approximately 5

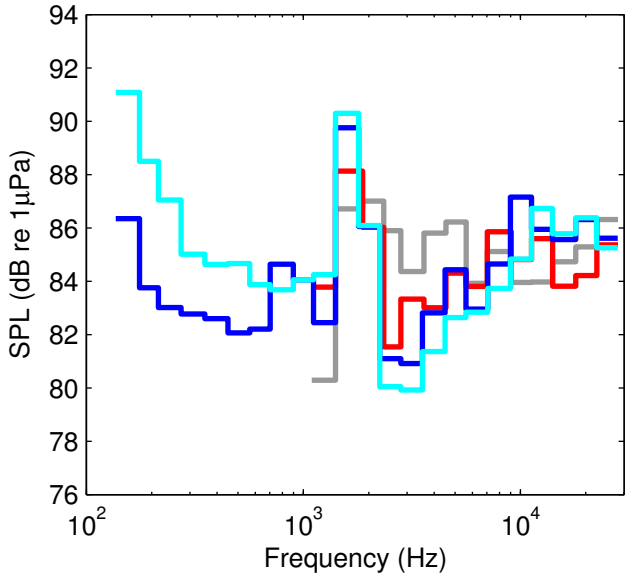

Fig. 9: Permanent noise spectra in one-third octave bands for each deployment. Plot lines colors correspond to the following deployments: 1-gray, 2-red, 3-blue, 4-light blue

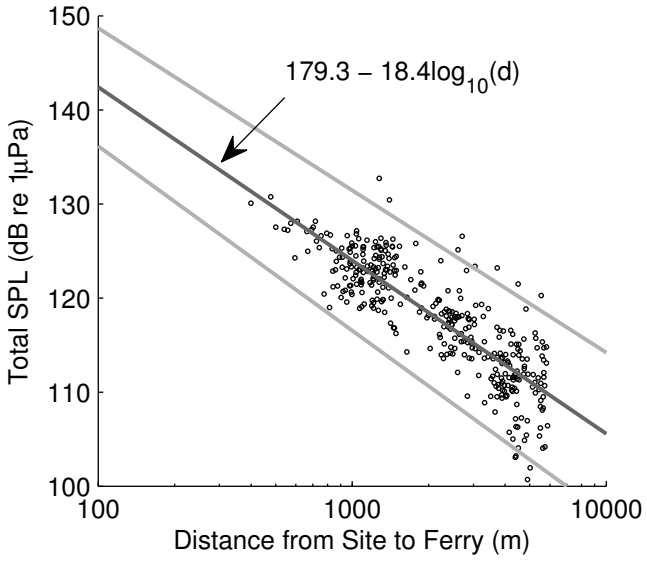

Fig. 10: Total sound pressure level versus distance from the ferry including ferry source level and spreading loss estimates with 95% confidence intervals.

nautical miles) are also removed in order to avoid contributions from other anthropogenic sources. The 9 km threshold ensures that any other ship identified by AIS is at least 2.5 km further from the site than the ferry terminal in Port Townsend. The resulting data set includes 368 unique recordings and ship locations used to estimate the ferry source level and spreading losses. A scatter plot of the data including 95% confidence intervals is included in Figure 10. The resulting estimated source level is 179 $\pm$ 4 dB at 1m and the spreading losses are estimated to be 18.4 $\pm$ 1.2 dB per order of magnitude increase in distance from the source.

D. Rain

The acoustic signature of light precipitation, a broad spectral peak around 15 kHz, can be identified in the absence of loud anthropogenic noise sources near the site or contamination by pseudosound. Acoustic spectra consistent with light rain are identified using a thresholding algorithm that searches for spectra in which pressure spectral densities are 4 dB louder at 15 kHz than at 9 kHz. The algorithm is adapted from a semi-empirical algorithm developed in Ma et al. (2005) for estimating underwater noise levels from precipitation rates and wind speeds. The dates of recordings with spectra consistent with light precipitation rates are compared with data hourly and daily precipitation data from the Washington State University Agricultural Network Weather station on Whidbey Island. Given that precipitation may fall at the weather station but not at the site, measurements from the site are only compared to days when precipitation was measured on Whidbey Island. Maximum daily precipitation rates recorded on Whidbey Island are used as a measure of the maximum precipitation rate at the site.

Given that the underwater noise produced by precipitation is well understood, the algorithm provides a measure of how often pressure spectral densities at the higher frequencies impacted by light rainfall are exceed by anthropogenic noise or masked by pseudosound. Table IV includes the number of days of rainfall reported at the weather station, how many days of rainfall were detected by the algorithm, and the percentage of days with precipitation were detected for different rainfall rates.

TABLE IV: Reported and detected precipitation

Maximum Precip. Rate	**Days Reported**	**Days Detected**	**Percent Detected**
$>$ 2 mm/hr	21	15	71
$>$ 1 mm/hr	47	32	68
$>$ 0.5 mm/hr	74	46	62
$<$ 0.5 mm/hr	33	10	30
$>$ 0 mm/hr	109	55	50
None	-	8	-

During the four deployments 21 days with rainfall rates greater than 2.0 mm/hr are reported and 15 days are detected. A total of 109 days of rainfall are reported but only 50 days are detected. The algorithm detects only 30% of days with rainfall rates less than 0.5 mm/hr. Eight additional days where no rainfall is reported are detected. This can be explained by the fact that lower precipitation rates are associated with smaller droplets that are less likely to entrain air and produce the acoustic signature of light rainfall [2]. The results suggest that periods of rainfall may, at times, be masked by anthropogenic noise sources or pseudosound but that transient events occurring in the 10-20 kHz range are typically detectable at

the site.

V. Conclusion

Passive acoustics data collected between May, 2009 to May, 2010 with a 1% duty cycle demonstrate that underwater noise conditions in Admiralty Inlet, WA are affected by a number of natural, biological, and anthropogenic sources. Anthropogenic sources are the most important contributors to the noise budget due to local ferry and shipping traffic. Integration of ancillary data sets about weather, ship traffic, and biological sources are necessary to explain underwater noise variability and to identify transient sources at the site.

Sites suitable for tidal hydrokinetic energy development are highly energetic and present unique challenges for proper measurement and quantification of underwater ambient noise. Pseudosound, non-propagating pressure fluctuations that are measured by hydrophones and can mask ambient noise, needs to be considered in such environments. In Admiralty Inlet, changes in the statistical distributions of total sound pressure levels and one-third octave bands sound pressure levels when currents exceed 1 m/s suggest pseudosound contamination.

Mean total sound pressure levels (0.156 - 30 kHz) for the year are 117 dB and mean total sound pressure levels between 116 dB and 118 dB for individual deployments. Total sound pressure levels are below 100 dB approximately 1% of the time and exceed 130 dB approximately 4% of the time. The minimum and maximum total sound pressure level recorded at the site are 94 dB and 144 dB respectively.

VI. Acknowledgments

Thanks to Snohomish Public Utility District for providing the funding to support a graduate research assistant on this project. Funding for field work and instrumentation was provided by the US Department of Energy. Thanks to Joe Talbert for designing, assembling and maintaing the instrument tripod throughout the deployments.

References

[1] G. Wenz, "Acoustic ambient noise in the ocean: Spectra and sources," *Journal of the Acoustical Society of America*, vol. 34, no. 12, pp. 1936–1956, 1962.

[2] B. Ma, J. Nystuen, and R.-C. Lien, "Prediction of underwater sound levels from rain and wind," *Journal of the Acoustical Society of America*, vol. 117, no. 6, pp. 3555–3565, June 2005.

[3] P. Wille and D. Geyer, "Measurements on the origin of the wind-dependent ambient noise variability in shallow water," *Journal of the Acoustical Society of America*, vol. 75, no. 1, pp. 173–185, January 1984.

[4] H. Medwin, J. Nystuen, P. Jacobus, and L. Ostwald, "The anatomy of underwater rain noise," *Journal of the Acoustical Society of America*, vol. 92, no. 3, pp. 1613–1623, September 1992.

[5] J. Nystuen and D. Farmer, "The influence of wind on the underwater sound generated by light rain," *Journal of the Acoustical Society of America*, vol. 82, no. 1, pp. 270–274, July 1987.

[6] J. Hildebrand, *Impacts of Anthropogenic Sound*. The Johns Hopkins University Press, Baltimore, Maryland, 2005.

[7] P. Arveson, "Radiated noise characteristics of a modern cargo ship," *Journal of the Acoustical Society of America*, vol. 107, no. 1, pp. 118–129, January 2000.

[8] D. Ross, *Mechanics of Underwater Noise*. Permagon Press, 1976.

[9] L. Gray and D. Greeley, "Source level model for propeller blade rate radiation for the world's merchant fleet," *Journal of the Acoustical Society of America*, vol. 67, no. 2, pp. 516–522, February 1980.

[10] P. Scrimger and R. Heitmeyer, "Acoustic source-level measurements for a variety of merchant ships," *Journal of the Acoustical Society of America*, vol. 89, no. 2, pp. 691–699, February 1991.

[11] J. Willis and F. Dietz, "Some characteristics of 25-cps shallow-water ambient noise," *Journal of the Acoustical Society of America*, vol. 37, no. 1, pp. 125–130, January 1965.

[12] R. Urick, *Principles of Underwater Sound for Engineers*. McGraw-Hill, Inc., 1967.

[13] N. Strasberg, "Nonacoustic noise interference in measurements of infrasonic ambient noise," *Journal of the Acoustical Society of America*, vol. 66, no. 5, pp. 1487–1493, November 1979.

[14] M. Strasberg, "Dimensional analysis of windscreen noise," *Journal of the Acoustical Society of America*, vol. 83, no. 2, pp. 544–548, February 1988.

[15] G. Deane, "Long time-base observations of surf noise," *Journal of the Acoustical Society of America*, vol. 107, no. 2, pp. 758–770, February 2000.

[16] M. Priestley, *Spectral Analysis and Time Series*. Academic Press, 1981.

[17] R. N. Bracewell, *The Fourier Transform and Its Applications*. McGraw-Hill, Inc., 2000.

[18] D. Dall'Osto, "A study of the spectral and directional properties of ambient noise in puget sound," Master's thesis, University of Washington, 2009.